Volume 21 | Issue 3 Article 3

2022

Uncertainty analysis of operational conditions in selective artificial ground freezing applications

Author(s) ORCID Identifier:
Ahmad Zueter 0000-0003-4521-3790
Saad Akhtar 0000-0001-5477-4974
Agus Sasmito 0000-0003-3444-8922

Uncertainty analysis of operational conditions in selective artificial ground freezing applications

Abstract

Artificial ground freezing (AGF) systems are susceptible to uncertain parameters highly affecting their performance. Particularly, selective artificial ground freezing (S-AGF) systems involve several uncertain operational conditions. In this study, uncertainty analysis is conducted to investigate four operational parameters: 1) coolant inlet temperature, 2) coolant flow rate, 3) pipes emissivity, and 4) pipes eccentricity. A reduced-order model developed and validated in our previous work for field-scale applications is exploited to simulate a total of 5,000 cases. The uncertain operational parameters are set according to Monte Carlo analysis based on field observations of a field-scale freeze-pipe in the mining industry extending to 460 m below the ground surface. The results indicate that the freezing time can range between 270 and 350 days with an average of 310 days, whereas the cooling load per one freeze-pipe ranges from 90 to 160 MWh, with an average of 129 MWh. Furthermore, it is observed that the freezing time and energy consumed are mostly dominated by the coolant inlet temperature, while energy dissipated in the passive zone (where ground freezing is not needed) is mostly affected by pipes emissivity. Overall, the conclusions of this study provide useful estimations for engineers and practitioners in the AGF industry.

Keywords

selective artificial ground freezing, Monte Carlo, pipes eccentricity, uncertainty analysis, reduced-order modelling

Uncertainty analysis of operational conditions in selective artificial ground freezing applications

Ahmad Zueter, Saad Akhtar, Agus Sasmito*

McGill University, Mining Engineering Department, Montreal, Quebec, Canada

Abstract

Artificial ground freezing (AGF) systems are susceptible to uncertain parameters highly affecting their performance. Particularly, selective artificial ground freezing (S-AGF) systems involve several uncertain operational conditions. In this study, uncertainty analysis is conducted to investigate four operational parameters: 1) coolant inlet temperature, 2) coolant flow rate, 3) pipes emissivity, and 4) pipes eccentricity. A reduced-order model developed and validated in our previous work for field-scale applications is exploited to simulate a total of 5000 cases. The uncertain operational parameters are set according to Monte Carlo analysis based on field observations of a field-scale freeze-pipe in the mining industry extending to 460 m below the ground surface. The results indicate that the freezing time can range between 270 and 350 days with an average of 310 days, whereas the cooling load per one freeze-pipe ranges from 90 to 160 MWh, with an average of 129 MWh. Furthermore, it is observed that the freezing time and energy consumed are mostly dominated by the coolant inlet temperature, while energy dissipated in the passive zone (where ground freezing is not needed) is mostly affected by pipes emissivity. Overall, the conclusions of this study provide useful estimations for engineers and practitioners in the AGF industry.

Keywords: selective artificial ground freezing, Monte Carlo, pipes eccentricity, uncertainty analysis, reduced-order modelling

1. Introduction

Artificial ground freezing (AGF) is widely employed to enhance the safety of mining systems by creating a solid impenetrable ground that stabilizes mine infrastructure [1–3] and contain mining contaminants [4]. Selective artificial ground freezing (S-AGF) is particularly useful in underground mining applications where the orebody is located hundreds of meters below the ground surface. The main advantage of S-AGF over other conventional AGF methods is the addition of air cavity to decrease heat gained by the coolant in the passive zone located away from the orebody. Accordingly, the required cooling load of the coolant decreases, resulting in more environmentally-friendly systems that minimize energy expenditures and greenhouse gas emissions [5]. Such S-AGF systems have been employed in the Cigar Lake Mine (Saskatchewan, Canada) [6] and the Banji Mine (Anhui, China) [7]. However, AGF systems involve several uncertain parameters that highly affect the progress of the frozen ground in the active zone, where ground freezing is desired, and the overall cooling load [8–10]. For instance, the cooling brine is provided at a variable range of temperatures and volume flow rates. Further, S-AGF applications are susceptible to additional uncertainty due to the air cavity installation difficulties. Typically, the air cavity is created by connecting 10-m-long piping segments over a depth of 400 m. While it is desired to form a concentric air cavity, as shown in Fig. 1(a), the middle pipes often collide with the casing in a zigzag profile, as shown in Fig. 1(b). The uncertain extent of the collision, as well as walls emissivity, can greatly impact the heat gained in the passive zone.

To better understand the impact of uncertain parameters in mining operations, several studies have conducted risk management supported with uncertainty analysis. Spandis et al. [11] proposed a novel

Received 30 March 2022; revised 15 July 2022; accepted 19 July 2022.
Available online 29 October 2022

* Corresponding author.
E-mail address: agus.sasmito@mcgill.ca (A. Sasmito).

https://doi.org/10.46873/2300-3960.1357

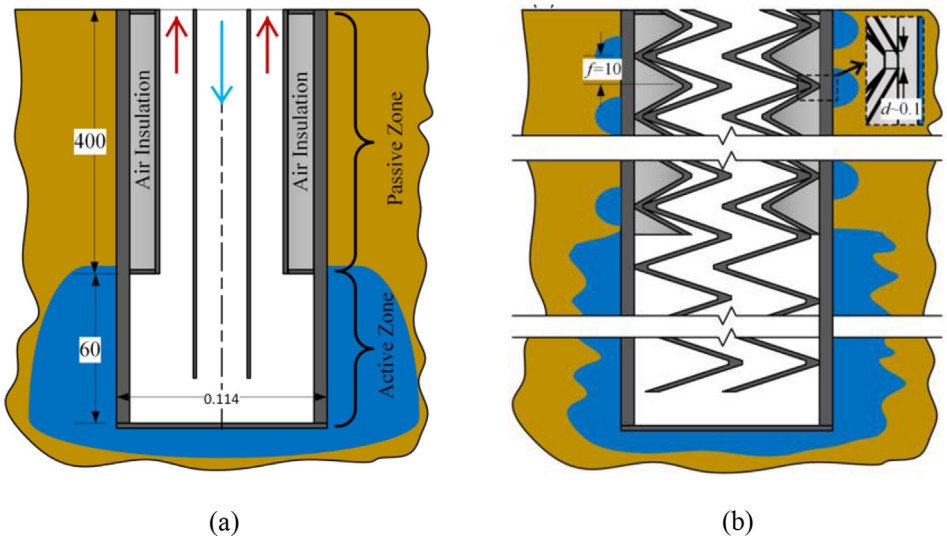

Fig. 1. Comparison between an ideal and unideal selective artificial ground freezing (S-AGF) system: (a) ideal system where all pipes are concentric around the same central axis; (b) unideal system where the inner and middle pipes zigzag along the casing due to installation difficulties. The arrows represent the coolant inlet and outlet. All dimensions are in meters (not-to-scale).[22] Received copyright permission from the ASME to reproduce this figure in this article.

methodology for risk assessment of surface mining natural hazards based on the triangular Fuzzy Analytical Hierarchy Process (FAHP). The FAHP process is also coupled with Monte Carlo simulation and the Program Evaluation Review Technique (PERT) method to predict uncertain outcomes. As for the uncertain analysis of AGF systems, most studies examined the effect of ground geological parameters on the growth of the frozen ground. Qiu et al. [12] modeled seepage flow considering variable ground thermal conductivity employing Monte-Carlo simulations. Wang et al. [13] added the uncertainty of the ground heat capacity and latent heat also using Monte-Carlo simulations based on 1D freezing models. Wang et al. [14] then carried out additional 1D freezing experiments to find the coefficient of variation (CoV) and scale of fluctuation (SoF) of uncertain hydrothermal properties including ground thermal diffusivity, moisture diffusivity, and freezing temperature. The CoV and SoF were utilized to formulate a stochastic hydrothermal model. Afterwards, Wang et al. [15] extended the stochastic model from 1D freezing around a single freeze-pipe to 2D freezing around a multi-circle freezing pipe. Besides geological uncertainties of the ground, Liu et al. [16] considered installation uncertainties, namely freeze-pipe inclination using Monte-Carlo analysis based on 3D freezing models.

In regards to S-AGF applications in particular, the literature is limited to experimental and mathematical studies that do not consider the various operational and installation uncertainties. Wang et al. [7] developed a numerical model for S-AGF to anticipate the frozen ground's expansion for the Banji Mine case. Vitel et al. [17] derived and validated a ground freezing model of S-AGF that particularly examines the active zone of the Cigar Lake Mine. Tounsi et al. [18] incorporated a mechanical model to estimate ground displacement associated with the ground freezing process in the active zone as well. Zueter et al. [6] conducted the first controlled experimental study of selective artificial ground freezing, associated with a mathematical model based on the enthalpy-porosity method [19,20]. Afterwards, Zueter et al. [21] developed reduced-order models for S-AGF applications to enhance the computational speed of field scenarios, which usually occupy large computational domain and operate for long periods. Zueter et al. [22] then employed the reduced-order model to examine the impact of freeze-pipe eccentricity on heat dissipation in the passive zone.

While the uncertainty of geological parameters has been addressed in the literature on AGF, several operational parameters and installation issues have not been examined, especially in S-AGF applications. Uncertainty of operational parameters brings about unpredictable energy consumption and freezing time of mines adopting S-AGF, such as the Cigar Lake Mine. This affects the associated costs and timeline of the mining operations. Accordingly, this study utilizes reliable conjugate models developed in our previous work [22] to understand the uncertain effect of operational and installation parameters on the frozen ground development and the cooling load of S-AGF applications. Particularly, the

study considered four main parameters not addressed in previous studies: 1) coolant inlet temperature, 2) coolant flow rate, 3) pipes emissivity, and 4) collision contact length between inner pipes and casing.

To this end, computationally efficient reduced-order models that have been derived and validated in our previous work [22] are utilized simulating a total of 5000 cases throughout this study. The article is organized as follows. In section 2, the mathematical model is shown as derived in our previous work [22]. After that, the input data to the Monte Carlo analysis are set in section 3. The results are presented in section 4, where the most likely frozen ground growth and cooling load are evaluated. Finally, the individual impact of uncertain parameters is analysed.

2. Materials and methods

A conjugate reduced-order numerical model developed in our previous work [22] is employed in the present study to monitor the frozen ground expansion in the active zone as well as the overall cooling load. This model is chosen due to its high computational efficiency, which is essential in this study for simulating 5000 cases. Furthermore, the model is based on a space-marching algorithm that monitors the evolution of the coolant thermal energy to evaluate the cooling load, as will be mathematically demonstrated in this section.

2.1. Governing equations and boundary conditions

The computational domain of the system is made up of a porous saturated ground surrounded by various boundaries. The governing equation of the ground thermal energy is based on a two-phase transient enthalpy method [23] given as

$$\frac{\partial H_g}{\partial t} = \nabla \cdot \left(k_g \nabla T_g\right) \tag{1}$$

where t, H_g, k_g, and T_g represent time, ground enthalpy, ground thermal conductivity, and ground temperature, respectively. In this study, the local thermal equilibrium assumption [24] between the sand particles and ground water content is considered valid, as demonstrated in our previous work [19,25]. The ground enthalpy is calculated based on the ground temperature as

$$H_g = (1-\gamma)\int_{T_{ref}}^{T_g} \left(\rho_g c_{p,g}\right)_f dT_g + \gamma \int_{T_{ref}}^{T_g} \left(\rho_g c_{p,g}\right)_u dT_g + \varphi\gamma\rho_w L_w \tag{2}$$

where $\rho_g c_{p,g}$ is the volumetric sensible heat capacity of the ground, $\rho_w L_w$ is the volumetric latent heat capacity of the water content, and T_{ref} is an arbitrary reference temperature. Subscripts f and u refer to ground frozen and unfrozen states, respectively. Further, φ denotes the ground porosity, whereas γ represents the liquid fraction of the water content calculated as

$$\gamma = \begin{cases} 0, & T_g < T_{sol} \\ \left(T_g - T_{sol}\right)/\left(T_{liq} - T_{sol}\right), & T_{sol} < T_g < T_{liq} \\ 1, & T_g > T_{liq} \end{cases} \tag{3}$$

where T_{liq} and T_{sol} represent the liquidus and solidus temperatures of the water content, respectively. In this study, the liquidus and solidus temperatures are set at 0 and $-0.50\,^{\circ}\mathrm{C}$ as per the experimental measurements of Zueter et al. [6]. The equivalent ground thermal conductivity is calculated based on the parallel arrangement approach [24] as

$$k_g = (1-\gamma)k_f + \gamma k_u \tag{4}$$

The ground is surrounded by several boundaries. Atmospheric convection is set along the top boundary of the domain along the ground surface, given as [26].

$$-k_g \frac{\partial T_{ground\ surface}}{\partial n} = h_{atm}\left(T_{ground\ surface} - T_{atm}\right) \tag{5}$$

where n is a vector perpendicular to the boundary, h_{atm} is the atmospheric heat transfer coefficient, and T_{atm} is the atmospheric temperature. Atmospheric temperature data of the Cigar Lake Mine is considered in this study fitted in a sinusoidal function as

$$T_{atm} = 267 - 21.3\cos\left(2\cdot 10^{-7}t\right) - 1.7\sin\left(2\cdot 10^{-7}t\right) \tag{6}$$

Geothermal heat flux is set at the bottom boundary of the domain as [26].

$$q_{geo} = -k_g \frac{\partial T_{bottom\ boundary}}{\partial n} \tag{7}$$

where $q_{geo} = 0.06\left[\frac{W}{m^2}\right]$. The axis of symmetry below the pipe is modeled considering zero thermal gradient perpendicular to the boundary [26] as

$$-k_g\frac{\partial T_{axis}}{\partial n}=0 \tag{8}$$

The distance between the freeze-pipe and the side boundary at the east of the computational is set according to the freeze-pipe spacing in fields. Typically, around 6 m is set between adjacent pipes; accordingly, each pipe is required to freeze a radial distance of 3 m. Thus, the east boundary is displaced 3 m away from the central axis of the freeze-pipe and is mathematically expressed considering zero thermal gradient as

$$-k_g\frac{\partial T_{east}}{\partial n}=0 \tag{9}$$

Mathematical modeling of the boundaries along the freeze-pipe in the active and passive zones is elaborately derived and presented in detail in our previous work [22]. Starting with the passive zone, given the very high aspect ratio of the air cavity in this study, the natural convection of air is negligible as compared to radiation and conduction [27]. The combined radiation and conduction heat transfer coefficient, $U_{passive}$, is derived as [22].

$$U_{passive}=\frac{Sk_{air}}{\pi(D_{out}+2\delta)}+\frac{D_{in}\varepsilon\sigma}{D_{out}+2\delta}\left(T_{g,passive}^2+T_c^2\right)\times\left(T_{g,passive}+T_c\right) \tag{10}$$

where the first and second terms on the right-hand side represent the contribution of conduction and radiation, respectively. Further, D_{out}, D_{in}, and δ denote the outer diameter of the air cavity, the inner diameter of the air cavity, and thickness of the casing. Also, T_c represents the coolant temperature, whereas the Greek symbols ϵ and σ denote pipes emissivity and Boltzmann radiation constant, respectively. S is the conduction shape factor that captures the eccentric impact of the air cavity expressed as [26].

$$S=2\pi\cosh^{-1}\left(\frac{D_{in}^2+D_{out}^2-4l}{2D_{in}D_{out}}\right) \tag{11}$$

where l is the linear eccentricity of the air cavity. The overall heat transfer coefficient, $U_{passive}$, is coupled to the computational domain along the freeze-pipe wall of the passive zone as

$$-k_g\frac{\partial T_{freeze\ pipe}}{\partial n}=U_{passive}\left(T_{freeze\ pipe}-T_c\right) \tag{12}$$

As for the active zone, convective heat extraction by the coolant is modelled following the analytical correlations of a laminar flow in an eccentric annular cavity derived in our previous work [22] (based on the analytical derivation of Michael and Trombetta [28]) as

$$h_{active}=F\left(3.4e^2-6.6e+4.9\right)k_c/\lambda \tag{13}$$

where k_c is the thermal conductivity of the coolant, λ is the characteristic length of the flow (which is equivalent to the difference between the casing inner diameter and the inner tube outer diameter), F is a correction factor to address the impact of the development of the flow thermal boundary layer ($F=1.5$ in the previous study [22]). Further, the variable e is defined as

$$e=\frac{d_i}{R_o-R_i} \tag{14}$$

where R_i is the outer radius of the inner tube, R_o is the inner radius of the casing, and d_i is the absolute distance between the centre of the casing and the centre of the inner tube. Coupling between the ground and freeze pipe at the active zone is modelled as

$$-k_g\frac{\partial T_{freeze\ pipe}}{\partial n}=h_{active}\left(T_{freeze\ pipe}-T_c\right) \tag{15}$$

Finally, the evolution of the coolant temperature along the freeze-pipe is calculated per unit length of the freeze-pipe using the first law of thermodynamics as

$$\Delta T_c=\frac{\pi D_{casing}\,q}{\dot{m}_c c_{p,c}} \tag{16}$$

where D_{casing} is the outer diameter of the casing, $\dot{m}_c$ is the coolant mass flow rate, and $c_{p,c}$ is the coolant specific heat. The heat flux, q, is determined by equation (12) in the passive zone and equation (15) in the active zone. All thermophysical properties of the ground and the coolant are based on field data and can be found in our previous work [22].

2.2. Numerical solution algorithm and numerical parameters

In this study, a total of 5000 simulations were conducted to understand better the impact of uncertain parameters in unideal S-AGF systems. Employing a fast computational algorithm is therefore essential to reduce the computational time of this study to a feasible level. Accordingly, a computationally efficient space marching algorithm developed in our previous work [21] for S-AGF systems is used in this study. This algorithm reduced the computational cost by more than 99% compared to traditional numerical solvers. In essence, the space marching algorithm is based on solving 1D radial grid-lines in series in the direction of the coolant flow (from the bottom of the pipe to

the top). Elaborate details on the solution algorithm can be found in our previous work [21].

The transient and spatial terms of the governing equations and boundary conditions are discretized using first-order and second-order accurate schemes. The numerical tolerance of the temperature field across the computational domain is set at 1E-5 K. Further, mesh and time-step independence are ensured in this study. Validation of the mathematical model against our own experimental data can be found in our previous work [22].

2.3. Monte Carlo simulations

Monte Carlo is a statistical algorithm aiming to find the most likely outcomes and numeric possibilities resulting from random parameters. Accordingly, the first step is to determine the random parameters of interest. In general, AGF applications involve several geological and operational parameters. Since several studies were conducted to examine the uncertainty of ground geological parameters (e.g., thermophysical properties of the ground), this study highlights the impact of uncertain operational parameters. In particular, the following parameters are considered in this study: 1) coolant inlet temperature, 2) coolant volume flow rate, 3) pipes emissivity, and 4) collision distance between inner pipes and casing.

The second step of Monte Carlo simulations is to determine the probability distribution of uncertain parameters. As observed in the industry, the coolant inlet ranges between −25 to −35 °C, whereas the volume flow rate ranges between 1.5 and 2.5 m^3/h. Further, pipes emissivity is unknown and can uniformly range between 0 and 1. The collision distance, d, also ranges uniformly between 0 and 1 m. The probabilistic distribution of these parameters is shown in Fig. 2. All simulations in this study are conducted using MATLAB/2019b.

3. Results and discussion

Artificial ground freezing systems are often designed to optimize the freezing time of the ground while minimizing the cooling load. Thus, in this study, Monte Carlo analysis is conducted to see the impact of uncertain operational parameters on the performance of AGF systems, namely the

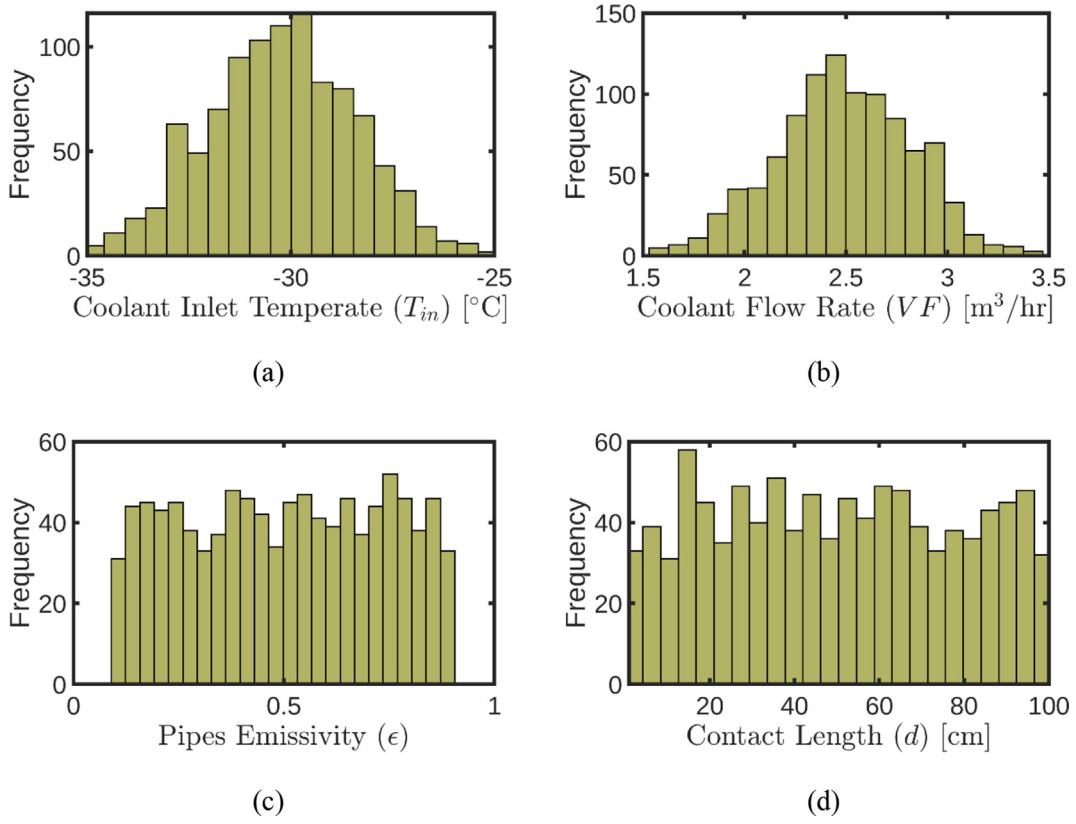

Fig. 2. Probabilistic distribution of uncertain parameters in the present study: a) coolant inlet temperature, b) coolant flow rate, c) pipes emissivity, and d) collision contact length.

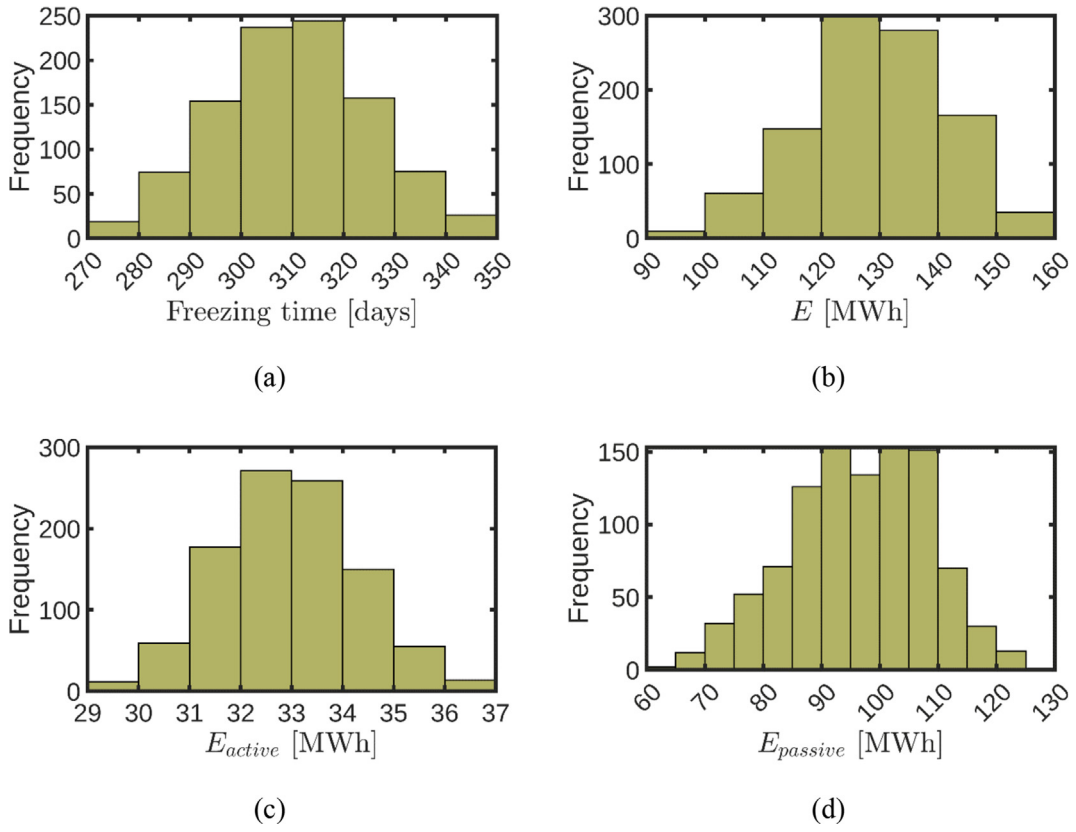

Fig. 3. Probabilistic distribution of output parameters for the first scenario: a) freezing time of the active zone, b) total cooling load, c) cooling load of the active zone, and d) cooling load of the passive zone.

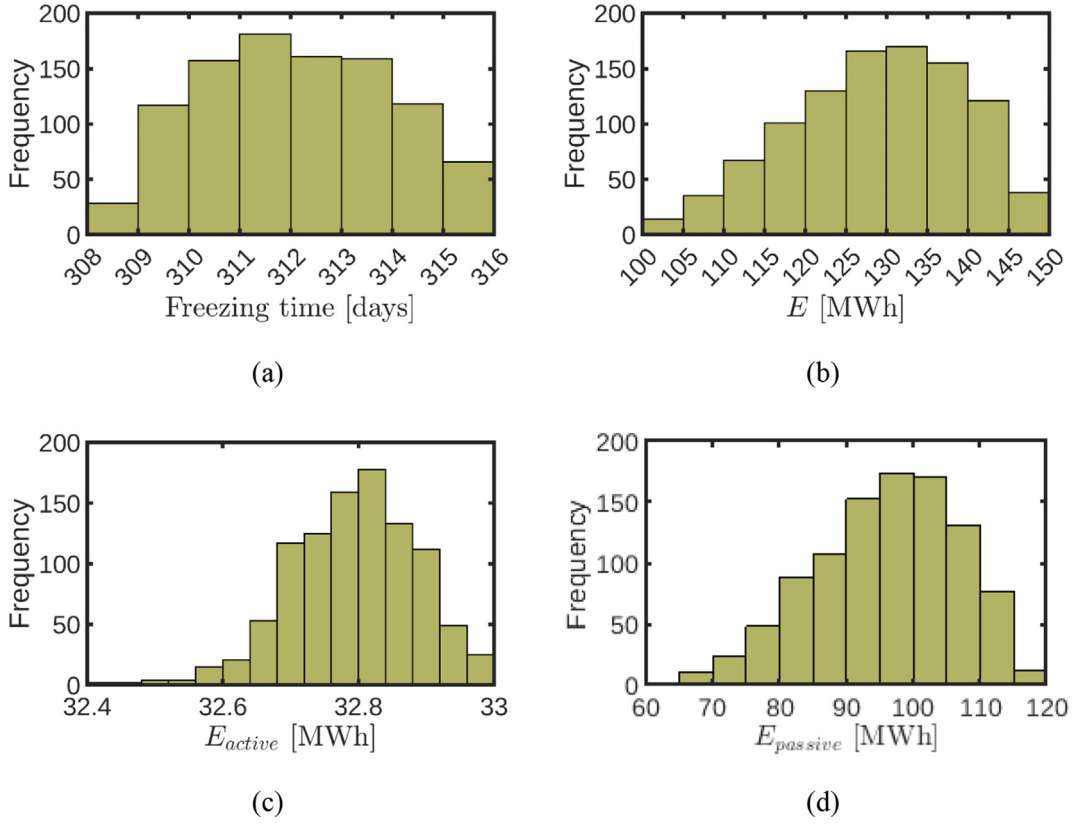

Fig. 4. Probabilistic distribution of output parameters for the second scenario: a) freezing time of the active zone, b) total cooling load, c) cooling load of the active zone, and d) cooling load of the passive zone.

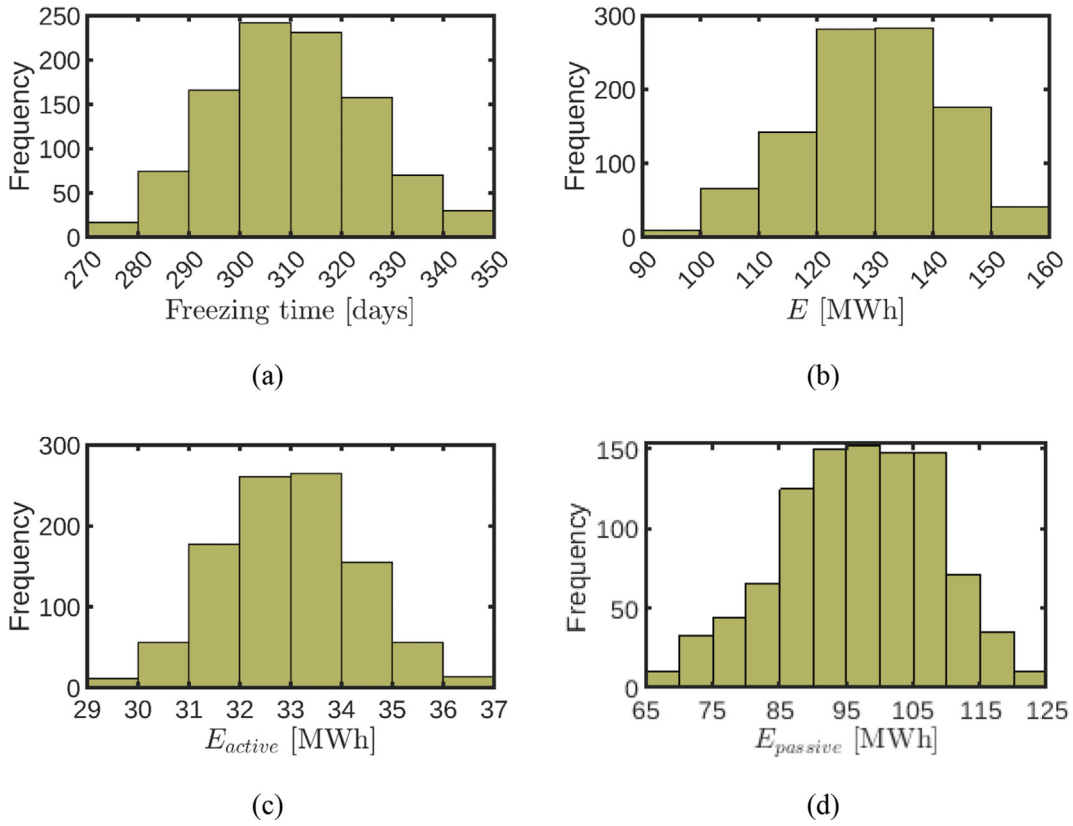

Fig. 5. Probabilistic distribution of output parameters for the third scenario: a) freezing time of the active zone, b) total cooling load, c) cooling load of the active zone, and d) cooling load of the passive zone.

Table 1. Statistical outcomes of scenario 1.

Statistical property	Freezing time [days]	E [MWh]	E_{active} [MWh]	$E_{passive}$ [MWh]
Average	310	129	33.0	96.4
Range	270–350	90–160	29–37	60–130
Standard deviation	17.2	12.3	1.39	11.7

freezing time and the cooling load. Five sets of simulations/scenarios are conducted, each of which for 1000 cases (total of 5000): 1) varying all input parameters, 2) fixing the coolant inlet temperature at −30 °C while varying other input parameters, 3) fixing the coolant flow rate at 2.5 m^3/h while varying other input parameters, 4) fixing the pipes emissivity at 0.5 while varying other input parameters, and 5) fixing the collision contact length to 5 cm while varying other parameters. The last four sets of

Table 2. Statistical outcomes of scenario 2.

Statistical property	Freezing time [days]	E [MWh]	E_{active} [MWh]	$E_{passive}$ [MWh]
Average	312	129	32.8	95.9
Range	308–316	100–150	32.4–33	60–120
Standard deviation	1.98	10.6	0.0930	10.7

Table 3. Statistical outcomes of scenario 3.

Statistical property	Freezing time [days]	E [MWh]	E_{active} [MWh]	$E_{passive}$ [MWh]
Average	310	130	33.0	96.7
Range	270–350	90–160	29–37	65–125
Standard deviation	17.2	12.3	1.39	11.7

Table 4. Statistical outcomes of scenario 4.

Statistical property	Freezing time [days]	E [MWh]	E_{active} [MWh]	$E_{passive}$ [MWh]
Average	310	130	33.0	97.2
Range	270–350	100–150	29–37	75–120
Standard deviation	17.2	9.17	1.39	8.33

Table 5. Statistical outcomes of scenario 5.

Statistical property	Freezing time [days]	E [MWh]	E_{active} [MWh]	$E_{passive}$ [MWh]
Average	308	118	33.0	84.8
Range	270–350	90–150	29–37	60–110
Standard deviation	16.7	11.2	1.40	10.6

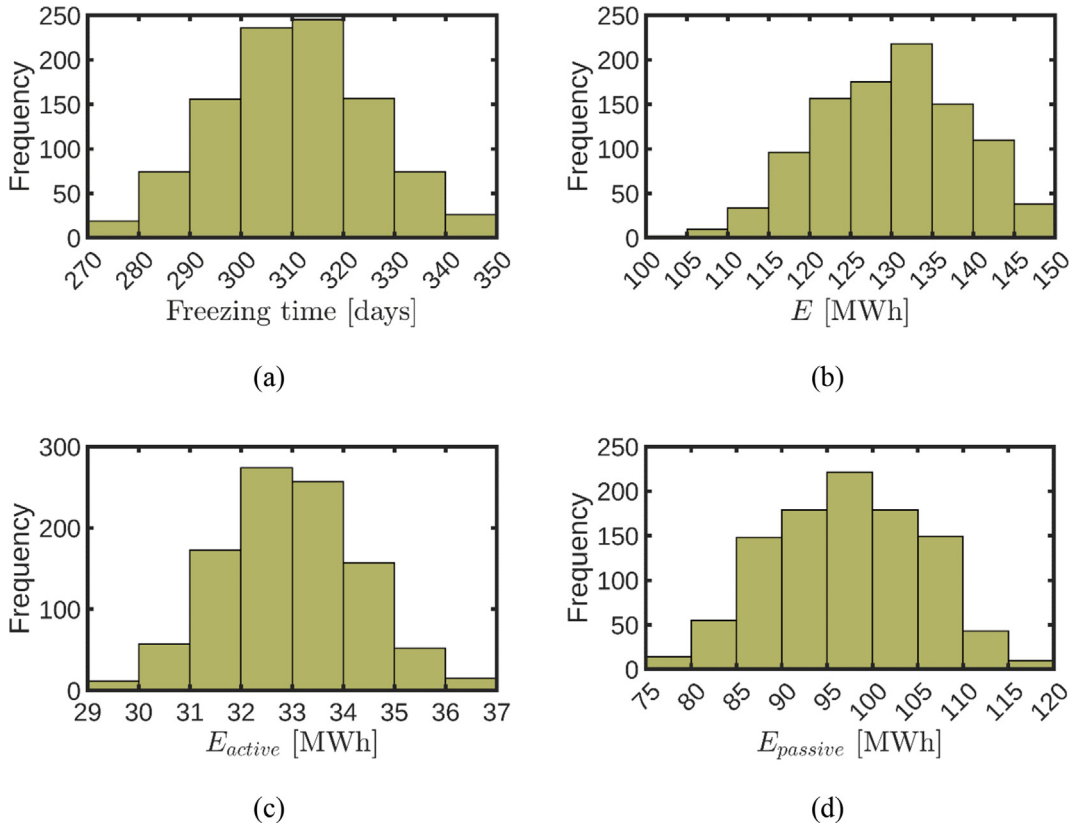

Fig. 6. Probabilistic distribution of output parameters for the fourth scenario: a) freezing time of the active zone, b) total cooling load, c) cooling load of the active zone, and d) cooling load of the passive zone.

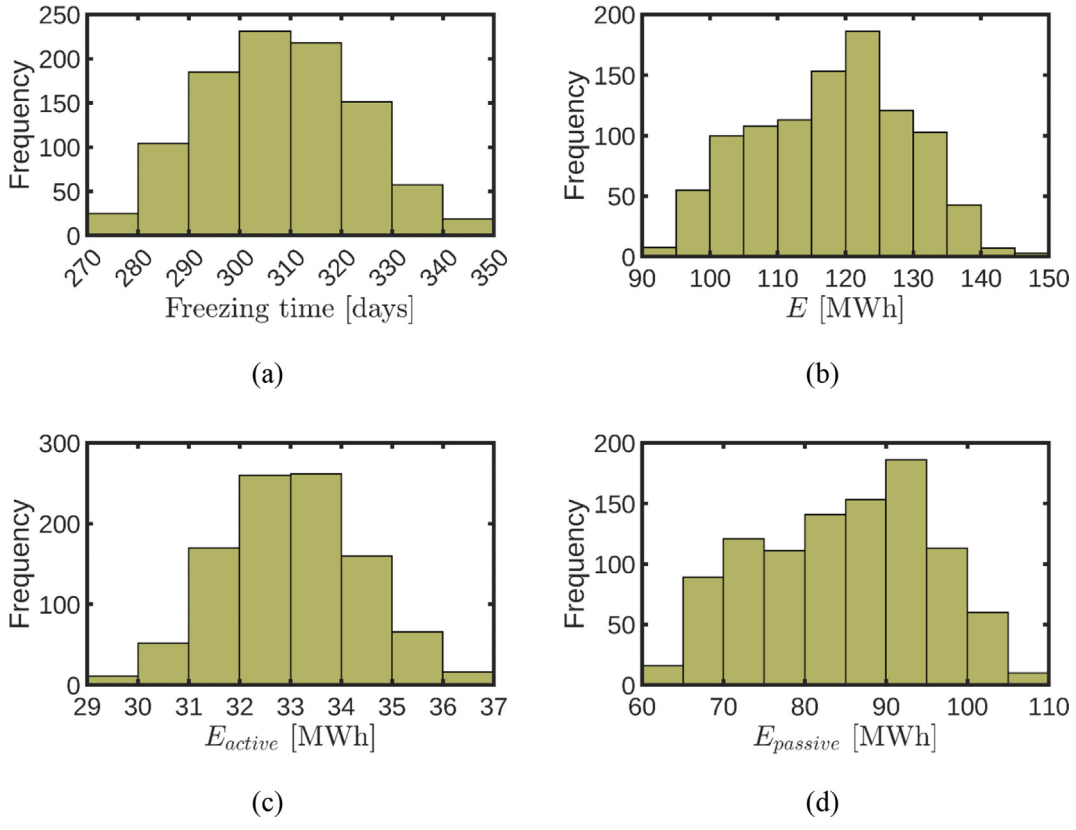

Fig. 7. Probabilistic distribution of output parameters for the fifth scenario: a) freezing time of the active zone, b) total cooling load, c) cooling load of the active zone, and d) cooling load of the passive zone.

simulations are conducted to understand each single variable impact on the outcomes' numeric probability.

3.1. Varying all input parameters (scenario 1)

First, all input parameters have been varied according to Fig. 2. As seen in Fig. 3, the freezing time is determined to range between 270 and 350 days, with an average of 310 days as shown in Table 1. Additionally, the cooling load required by one freeze-pipe coarsely ranges between 90 and 160 MWh at an average of 129 MWh. Despite the insulation layer in the passive zone, the average of energy consumed in the passive zone is three times higher than that of the active zone due to the larger extent of the passive zone (400 m) compared to the active zone (60 m). Particularly, the energy consumed in the passive zone ranges from 60 to 130 MWh at an average of 96 MWh, as compared to a range of 29–37 MWh with an average of 33 MWh in the active zone.

The asymmetric data distribution is observed in Fig. 3(d), describing the energy dissipated in the passive zone. In turn, this results in asymmetric data distribution in Fig. 3(b), which describes the total energy consumption per one freeze pipe as the sum of energy dissipated in the passive zone (shown in Fig. 3(d)) with that in the active zone (shown in Fig. 3(c)). Specifically, the results are somewhat skewed to the left. As the skewness in the total energy consumed is attributed to the passive zone rather than the active zone, the asymmetric behaviour is most likely attributed to the uncertainty of pipes emissivity or collision contact length as these parameters influence the passive zone only without any effect in the active zone. Accordingly, the skewness of total energy distribution is also observed in Fig. 4(b) and Fig. 5(b), where the coolant temperature and flow rate are fixed.

3.2. Fixing coolant inlet temperature (scenario 2)

In this subsection, the coolant inlet temperature is fixed at −30 °C to observe its impact with respect to other random parameters. First, it is observed that the range of the freezing time has substantially decreased, implying that the random variation of the coolant inlet temperature substantially affects the freezing time. Particularly, after fixing the coolant inlet temperature, the range has decreased from 80 days (270 days → 350 days) to eight days only (308 days → 316 days). Accordingly, the standard deviation of the freezing time also decreased from 17.2 days to 1.97 days only as shown in Table 2.

The energy consumed by each freeze-pipe is also found to be somewhat affected by the variation of the coolant inlet temperature. Particularly, the standard deviation after fixing the coolant inlet temperature has decreased from to 12.3 to 10.6 MWh. Most of this difference in the cooling load occurs due to variation in the energy consumed in the active zone rather than the passive zone. The standard deviation of the active zone cooling load in scenario 2 is 15 times lower than that of scenario 1, compared to 1.1 times only in the passive zone.

3.3. Fixing coolant flow rate (scenario 3)

In this subsection, the coolant flow rate is fixed at 2.5 m^3/h. Unlike the previous scenario, fixing the volume flow rate has almost no effect on the freezing time and energy consumed in the active. This is implied by the identical statistical outcomes of scenario 1 and scenario 3. The same observation is also noted in the passive zone. Comparing the standard deviations of both zones in Table 1 and Table 3, they all share the same values for all outcomes.

3.4. Fixing pipes emissivity (scenario 4)

In this subsection, the pipes emissivity is fixed at 0.5 while varying all other parameters. Evidently, the freezing time and energy consumed in the passive zone are not affected by pipes emissivity because radiation heat transfer only takes part in the passive zone. However, energy consumed in the passive zone is mostly affected by the emissivity as compared to other uncertain input parameters. Specifically, the standard deviation of energy consumed in the passive zone has decreased from 11.7 to 8.33 MWh as shown in Table 4.

Unlike the previous two scenarios, this scenario of fixing pipes emissivity features a more symmetric energy distribution in the total energy consumed (Fig. 6(b)) as well as energy dissipated in the passive zone (Fig. 6(d)). This demonstrates the role of the pipes emissivity in causing an asymmetric distribution of energy data as noted in Fig. 3(b), Fig. 4(b), Fig. 5(b), and Fig. 7(b). This could be attributed to the high incremental impact of pipes emissivity at low levels (i.e., 0 to 0.5) compared to that at higher levels. The higher incremental impact of pipes emissivity at lower levels causes the energy data distribution to be skewed to the left.

3.5. Fixing collision contact length (scenario 5)

In the last subsection, the collision contact length between the inner pipes and the casing is fixed at

5 cm while varying all others. The results reveal that the uncertainty of the collision contact length mildly affects the freezing time as well as energy consumed in the passive zones. Specifically, the standard deviation of the freezing time has decreased from 17.2 to 16.7 days as shown in Table 5. In addition, the standard deviation of energy consumed in the passive zone has decreased from 11.7 to 10.6.

4. Conclusions

In this study, the impact of four uncertain operational parameters in selective artificial ground freezing applications is examined: 1) coolant inlet temperature, 2) coolant flow rate, 3) pipes emissivity, and 4) collision contact length due to inner pipes eccentricity. A total of 5000 simulations are conducted using Monte Carlo analysis with the aid of field data to determine the distribution of uncertain input parameters. The Monte Carlo simulations are based on a computationally efficient reduced-order model developed and validated in our previous work [22]. Particularly, five sets of simulations are conducted (1000 simulations each): 1) varying all uncertain input parameters, 2) fixing the coolant inlet temperature while varying other parameters, 3) fixing the coolant flow rate while varying other parameters, 4) fixing pipes emissivity while varying other parameters, and 5) fixing the collision contact length while varying other parameters. The main results and findings are listed below:

- The results of the first set of simulations indicate that the freezing time can range between 270 and 350 days with an average of 310 days, whereas the energy consumed per one freeze-pipe ranges from 90 to 160 MWh, with an average of 129 MWh.
- The results of the second set of simulations demonstrate that the energy consumed in the active zone, as well as the freezing time, is mostly dependent on the uncertain behaviour of the coolant inlet temperature.
- In the third set of simulations, it is observed that uncertainty of the volume flow rate has a negligible impact on the freezing rate and energy consumed.
- The fourth set of simulations reveals that energy dissipated in the passive zone is mostly affected by the uncertainty of pipes emissivity.
- In the final set, it is observed that freeze-pipe eccentricity mildly affects the freezing rate and energy consumption.

In our future work, we aim to integrate the uncertainty of ground geological parameters alongside with the operational ones considered in this study. Ultimately, we aim to obtain a clear understanding of the most influential parameters of S-AGF under operational and geological conditions. This analysis is useful for mining industries to properly estimate the required freezing time and operational costs of S-AGF.

Ethical statement

The authors state that the research was conducted according to ethical standards.

Funding body

The authors would like to thank the FRQNT Development Durable du Secteur Minier-II (Grant No. 2020-MN-284402) Neumans Geotechnique Incorporation and Ultra Deep Mining Network (UDMN) (241695 Tri-Council (NCE–UDMN) 2-003). The first author wishes to thank the McGill Engineering Doctoral Award (MEDA) and the FRQNT Doctoral award (Grant No. 2021-B2X-306519), in addition to the graduate excellence awards of the mining department of McGill University.

Conflict of Interest

The authors declare no conflict of interest.

References

[1] Alzoubi MA, Xu M, Hassani FP, Poncet S, Sasmito AP. Artificial ground freezing: a review of thermal and hydraulic aspects. Tunn Undergr Space Technol 2020;104:103534.
[2] Harris JS. Ground freezing in practice. Thomas Telford; 1995.
[3] Sarkkinen M, Kujala K, Gehör S. Efficiency of MgO activated GGBFS and OPC in the stabilization of highly sulfidic mine tailings [Internet] J Sustain Min 2019;18(3):115–26. Available from: https://doi.org/10.1016/j.jsm.2019.04.001.
[4] Zueter AF, Newman G, Sasmito AP. Numerical study on the cooling characteristics of hybrid thermosyphons: case study of the Giant Mine, Canada [Internet] Cold Reg Sci Technol 2021;189 (February):103313. Available from: https://doi.org/10.1016/j.coldregions.2021.103313.
[5] Newman G, Newman L, Chapman D, Harbicht T. Artificial ground freezing: an environmental best practice at Cameco's Uranium mining operations in northern Saskatchewan, Canada. Ger: Mine Water—Managing Challenges Int Mine Water Assoc Aachen; 2011. p. 113–8.
[6] Zueter A, Nie-Rouquette A, Alzoubi MA, Sasmito AP. Thermal and hydraulic analysis of selective artificial ground freezing using air insulation: experiment and modeling. Comput Geotech 2020;120:103416.
[7] Wang B, Rong C, Cheng H, Yao Z, Cai H. Research and application of the local differential freezing technology in deep alluvium. Adv Civ Eng 2020:2020.
[8] Luo Z, Hu B, Wang Y, Di H. Effect of spatial variability of soft clays on geotechnical design of braced excavations: a case study of Formosa excavation [Internet] Comput Geotech 2018;103(January):242–53. Available from: https://doi.org/10.1016/j.compgeo.2018.07.020.
[9] Pan Y, Shi G, Liu Y, Lee FH. Effect of spatial variability on performance of cement-treated soil slab during deep

excavation [Internet] Construct Build Mater 2018;188:505–19. Available from: https://doi.org/10.1016/j.conbuildmat.2018.08.112.
[10] Pan Y, Liu Y, Xiao H, Lee FH, Phoon KK. Effect of spatial variability on short- and long-term behaviour of axially-loaded cement-admixed marine clay column [Internet] Construct Build Mater 2018;94:150–68. Available from: https://doi.org/10.1016/j.compgeo.2017.09.006.
[11] Spanidis PM, Roumpos C, Pavloudakis F. A fuzzy-ahp methodology for planning the risk management of natural hazards in surface mining projects. Sustain Times 2021;13(4):1–23.
[12] Qiu P, Li P, Hu J, Liu Y. Modeling seepage flow and spatial variability of soil thermal conductivity during artificial ground freezing for tunnel excavation. Appl Sci 2021;11(14).
[13] Wang T, Zhou G, Wang J, Zhou L. Stochastic analysis of uncertain thermal parameters for random thermal regime of frozen soil around a single freezing pipe. Heat Mass Tran 2018;54(9):2845–52.
[14] Wang T, Liu Y, Zhou G, Wang D. Effect of uncertain hydro-thermal properties and freezing temperature on the thermal process of frozen soil around a single freezing pipe [Internet] Int Commun Heat Mass Tran 2021;124(April):105267. Available from: https://doi.org/10.1016/j.icheatmasstransfer.2021.105267.
[15] Wang T, Zhou G, Xu D, Wang D, Wang J. Field experiment and stochastic model of uncertain thermal processes of artificial frozen wall around multi-circle freezing pipe [Internet] Int J Therm Sci 2021;160(October 2019):106658. Available from: https://doi.org/10.1016/j.ijthermalsci.2020.106658.
[16] Liu Y, Li KQ, Li DQ, Tang XS, Gu SX. Coupled thermal–hydraulic modeling of artificial ground freezing with uncertainties in pipe inclination and thermal conductivity [Internet] Acta Geotech 2022;17(1):257–74. Available from: https://doi.org/10.1007/s11440-021-01221-w.
[17] Vitel M, Rouabhi A, Tijani M, Guérin F. Thermo-hydraulic modeling of artificial ground freezing: application to an underground mine in fractured sandstone. Comput Geotech 2016;75:80–92.
[18] Tounsi H, Rouabhi A, Tijani M, Guerin F. Thermo-hydro-mechanical modeling of artificial ground freezing: application in mining engineering. Rock Mech Rock Eng 2019;1–19.
[19] Alzoubi MA, Nie-rouquette A, Sasmito AP. International Journal of Heat and Mass Transfer Conjugate heat transfer in artificial ground freezing using enthalpy-porosity method : experiments and model validation [Internet] Int J Heat Mass Tran 2018;126:740–52. Available from: https://doi.org/10.1016/j.ijheatmasstransfer.2018.05.059.
[20] Voller VR, Prakash C. A fixed grid numerical modelling methodology for convection-diffusion mushy region phase-change problems. Int J Heat Mass Tran 1987;30(8):1709–19.
[21] Zueter AF, Xu M, Alzoubi MA, Sasmito AP. Development of conjugate reduced-order models for selective artificial ground freezing: thermal and computational analysis. Appl Therm Eng 2021;190:116782.
[22] Zueter AF, Madiseh AG, Hassani FP, Sasmito AP. Effect of freeze pipe eccentricity in selective artificial ground freezing applications. ASME J Therm Sci Eng Appl 2022;14:011015.
[23] Swaminathan CR, Voller VR. A general enthalpy method for modeling solidification processes. Metall Trans B 1992;23(5):651–64.
[24] Kaviany M. Principles of heat transfer in porous media. Springer Science & Business Media; 2012.
[25] Alzoubi MA, Sasmito AP, Madiseh A, Hassani FP. Freezing on demand (FoD): an energy saving technique for artificial ground freezing. In: Energy procedia. Elsevier; 2019. p. 4992–7.
[26] Cengel YA, Klein S, Beckman W. Heat transfer: a practical approachvol. 141. New York: McGraw-Hill; 1998.
[27] Bejan A. Convection heat transfer. John Wiley & Sons; 2013.
[28] TM L. Laminar forced convection in eccentric annuli. J Chem Inf Model 1970;14:1161–73.